# PAPER K

# *CALCULATION OF DIRECT ARRIVAL TRAVELTIMES BY THE EIKONAL EQUATION*

Le-Wei Mo


## *ABSTRACT*

We present a traveltime calculation scheme based on the eikonal equation that calculates the traveltimes of direct arrivals from a point source. In typical earth models, critical refractions, diffractions and reflections are weak. Most of the energy radiated by the source is contained in the direct arrivals. Direct arrivals are thus generally the most energetic events in a time evolving wavefield. Our scheme successfully computes the traveltimes of direct arrivals and is computationally efficient. The method is presented in two dimensions.


## *INTRODUCTION*

Wave propagation in medium, in high frequency asymptotics, can be described by the WKBJ Green function, which consists of traveltimes and amplitudes. The traveltimes satisfy the eikonal equation that relates the gradient of the traveltimes to slowness of the model. The amplitudes satisfy the transport equations. In this paper, we will address the problem of solving the eikonal equation for direct arrival traveltimes. One method of solving the eikonal equation is the method of characteristics (Cerveny et al., 1977; Zauderer, 1989). The ray equations are derived from the eikonal equation, whose solutions are raypaths or the characteristic curves of the eikonal equation. Because the raypaths are local, wave propagation along rays is thus intuitive and easy to understand. This explains why the application of ray tracing is so popular and well published. However, ray tracing has its limitations and disadvantages as pointed out by some authors (Vidale, 1988). Seismic depth migration, and many other applications require traveltimes on a uniform grid. If these traveltimes are computed by ray tracing, computation cost is immense (Zhang, 1993). We would rather solve the eikonal equation directly for traveltimes on a uniform grid.

Reshef and Kosloff (1986) first formulated finite-difference scheme to solve the eikonal equation for traveltimes on a uniform grid by extrapolating the depth gradient of traveltimes. Vidale (1988, 1990) formulated a finite-difference scheme in Cartesian coordinates that solves the eikonal equation progressing outward from an "expanding square" for traveltimes of first arriving waves from a point source. His scheme can quickly fill in traveltimes in a uniform grid, and is by far the fastest method of computing traveltime. However, Vidale's scheme encounters stability problems, e.g., calculating the square root of a negative number. Qin et al. (1992) propose an alternate of Vidale's scheme, i.e., progressing outward from an "expanding wavefront." Qin et al.'s scheme solves some of the stability problems of Vidale's algorithm. But searching for the global minimum to start computation at each step makes their scheme very computation costly. Podvin and Lecomte (1991) dissect wave propagation in a cell into all possible modes of transmission, diffraction and head waves, resulting in a stable scheme of traveltime calculation. In their parallel implementation of traveltime calculation, each grid point of a velocity model is associated with a processor. All the processors simultaneously update the traveltimes at the associated grid point. However, traveltime calculation is a bad candidate for parallel computation. The parallel implementation does not effectively use computational power because, during the computation, most of the processors away from the wavefront perform useless operations. Van Trier and Symes (1991) and Zhang (1993) formulated traveltime calculation in polar coordinates by extrapolating the gradients of traveltimes. In their schemes, traveltime computation has the contradiction of dense sampling near the source and coarse sampling far away from the source. And mapping the slowness and traveltime fields to and from polar coordinates gives additional cost to their schemes. As a matter of fact, efficiency of a traveltime computation scheme also depends on the computer architecture. But Vidale's scheme requires the least number of algebraic operations.

The common shortcoming of the above finite-difference traveltime calculation schemes is that they all explicitly or implicitly calculate traveltime of first arriving waves, which may carry little energy and are quite weak, e.g., head waves and diffractions. In this paper, we propose a traveltime calculation scheme that aims at calculating the traveltimes of direct arrivals from a point source. In typical earth models, diffraction and reflection effects are weak. Most of the energy radiated by the source is contained in the direct arrivals. Direct arrivals are thus generally the most energetic events in a time evolving wavefield. First, we analyze why we prefer direct arrival traveltimes to first arriving traveltimes in tomography and migration imaging. Then we present our scheme of calculating direct arrival traveltimes. Finally, we show several numerical examples of calculating direct arrival traveltimes. Our scheme successfully computes the traveltimes of direct arrivals and is computationally efficient. The method is presented in two dimensions.

## *WHY DIRECT ARRIVAL TRAVELTIMES*

Figure 1(b) shows the snapshot wavefield at 0.16 seconds of a two layer velocity model of Figure 1(a). The wavefield is simulated by the finite-difference solution to the scalar wave equation. The source is at the upper left corner. The source wavelet is the first derivative of the Gaussian function. For this model, head wave is generated and part of its travel path is the boundary separating the slow and the fast medium. The head wave is a boundary wave, and carries very little energy. Figure 1(c) is the common shot gather or history wavefield of receivers at the right edge of Figure 1(b). From Figure 1(b) and (c), we see that the first arrival - head wave, travels ahead of the direct arrival and is much weaker than the direct arrival. If the traveltimes of the head wave in the slow medium were used for transmission traveltime tomography, the slow velocity medium would be inverted as an erroneous high velocity medium. And reflections that are used by migration to image velocity discontinuities are not generated by the first arrival head wave. Thus traveltimes of the first arrival - head wave, are not suited for transmission traveltime tomography and migration imaging. Instead, traveltimes of direct arrivals should be used. Overlay on Figure 1(b) and (c) are the direct arrival traveltimes computed by our finite-difference scheme of solving the eikonal equation. The direct arrival traveltimes closely match the first breaks of the direct arrivals computed by finite-difference wave equation modeling.

## *RAY TRACING*

Figure 2 is a two layer velocity model. The lower medium has higher velocity. By ray tracing, the incidence ray at point *C* is in critical incidence and generates a creeping ray along the boundary. The incidence rays to the left of point *C*, e.g., at point *A*, are in pre-critical incidence and generate refracted waves in the lower medium. The incidence rays to the right of point *C*, e.g., at point *B*, are in post-critical incidence, and total reflection occurs. For post-critical incidence rays, the symptoms are the sine of the refraction angle is greater than *1* and the incidence wavefront in the slow medium and the creeping wavefront in the fast medium are discontinuous across the interface. Transmission ray tracing can be performed for pre-critical incidence rays to the left of point *C*. However, transmission ray tracing can not be performed for post-critical incidence rays to the right of point *C*. That is, transmission ray tracing is performed only until total reflection occurs, or until the sine of the refraction angle is greater than *1*.

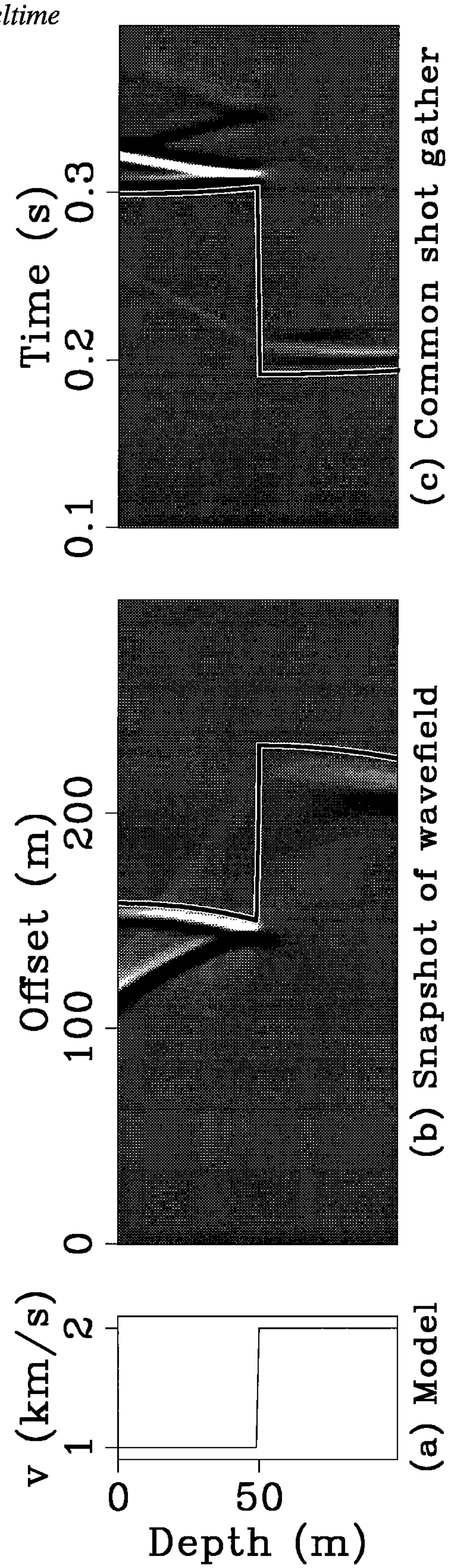


Figure 1: (a) is the velocity. In (b), source is at the upper left corner. (c) is the common shot gather with receivers at the right edge (b).

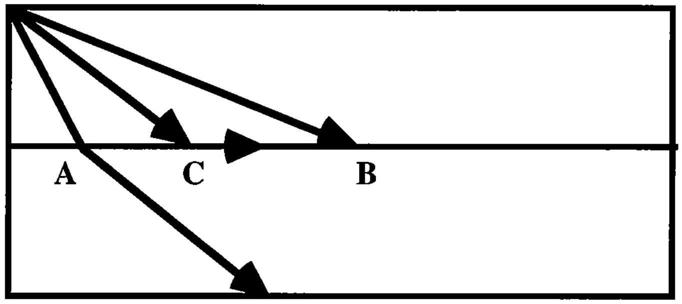


Figure 2: Incidence ray at point $C$ is in critical incidence. Incidence ray at $A$ ($B$) is in pre-critical (post-critical) incidence.

## *SOLVING THE EIKONAL EQUATION*

In a two dimensional medium, the traveltime of wave propagation is governed by the eikonal equation, which relates the gradient of traveltimes to the slowness of the medium,

$$\left(\frac{\partial t}{\partial x}\right)^2 + \left(\frac{\partial t}{\partial z}\right)^2 = s^2(x,z) \tag{1}$$

where $(x,z)$ is spatial coordinate, $t$ is traveltime, $s(x,z)$ is slowness. We parameterize the medium by square cells, with mesh spacing $h$, Figure 3. In a localized cell of Figure 3, when traveltimes at three corners $a$, $b$ and $c$ are known, the traveltime at the fourth corner --- $d$ can be found by finite-difference method based on the assumption of local plane wave. We use the centered finite-difference (Vidale, 1988) to approximate the two differential terms in equation (1)

$$\frac{\partial t}{\partial x} = \frac{1}{2h}\left(t_b + t_d - t_a - t_c\right) \tag{2}$$

and

$$\frac{\partial t}{\partial z} = \frac{1}{2h}\left(t_c + t_d - t_a - t_b\right) \tag{3}$$

Substituting equations (2) and (3) into equation (1) gives

$$t_d = t_a + \sqrt{2(hs)^2 - (t_b - t_c)^2} \tag{4}$$

where $h$ is mesh spacing, $s$ is the slowness inside the cell with the grid indexes of corner $d$, $t_a$, $t_b$, $t_c$ and $t_d$ are the traveltimes at the corners $a$, $b$, $c$ and $d$. Finite-differences in equations (2) and (3) have second order of numerical accuracy.

Equation (4) can only be used for traveltime calculation at pre-critical incidence. At post-critical incidence, the problem is to compute the square root of a negative number. But setting the negative number inside the square root to zero (Vidale, 1988, 1990) does not conform to physics. When geometrical ray theory is valid and the wavefronts are continuous across an interface, the time difference between diagonal nodes of a square cell is at most $\sqrt{2}hs$, where $h$ is the mesh spacing of the cell and $s$ is the slowness inside the cell. Thus there are three equivalent symptoms of post-critical incidence, the sine of the refraction angle being greater than *1*, wavefronts being discontinuous across an interface and the time difference between diagonal nodes of a square cell being greater than $\sqrt{2}hs$. Thus in solving the eikonal equation, the term inside the square root of equation (4) is negative at post-critical incidence. If corners $a$ and $b$ lie in a horizontal direction and wave travels from $a$ to $b$, then corners $a$ and $b$ are in the slow velocity medium, and corners $c$ and $d$ are in the high velocity medium. In geometric ray theory, the direct arrival to corner $d$ is a creeping ray from corner $c$ to corner $d$. The traveltime at corner $d$ is then computed as

$$t_d = t_c + hs \tag{5}$$

If corners $a$ and $b$ lie in a vertical direction and wave travels from $a$ to $b$, the direct arrival to corner $d$ is a creeping ray from corner $b$ to corner $d$. The traveltime at corner $d$ is then computed as

$$t_d = t_b + hs \tag{6}$$

We have described the traveltime computation at a localized cell. Next, we describe the arrangement of computation patterns.

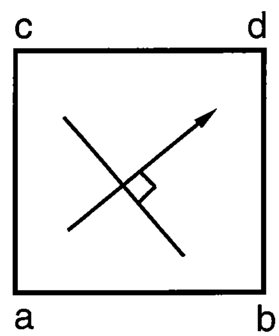


Figure 3: In a square cell with constant slowness *s*, wave propagates from corner *a* to corner *d* through corners *b* and *c*. *Traveltime* is larger at corner *b* than at corner *a*.

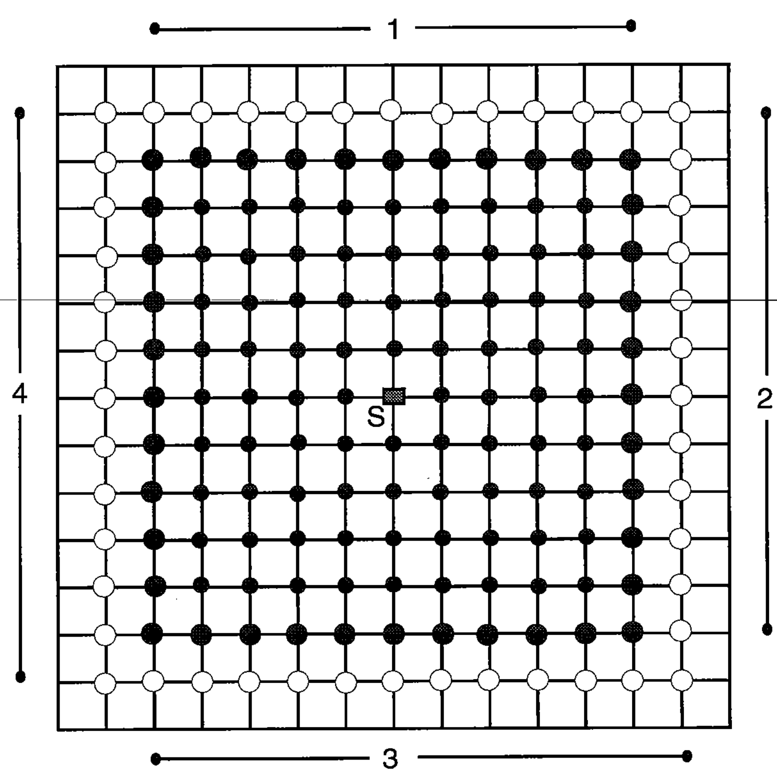


Figure 4: **S** is the source grid point. Traveltime computations proceed sequentially on the four sides.

Computation pattern

Traveltime computation is initialized by assuming straight ray paths in a constant velocity square surrounding the source point. We found the radius of $5h$ to be a generally good choice for the initialization square. Traveltime computations are then carried out by expanding squares around the source point, as the computation layout in Figure 4. The filled circles indicate grid points that have had their traveltimes calculated. We are to use the traveltimes at the boundary ring of grid points, large filled circles, to compute traveltimes of grid points at an outer ring, the hollow circles. The inductive scheme for calculating a new ring of traveltimes is now described. Computations proceed sequentially on the four sides, as shown in Figure 4. To initialize computation at a side, the points in the inner side are examined in a loop from one end to the other to locate the point with local minimum traveltime. Using one-sided finite-difference stencil, the traveltime of the point outside the point with local minimum traveltime is computed as

$$t_c = t_a + \sqrt{(hs)^2 - (t_b - t_a)^2} \tag{7}$$

where $t_c$ is the time to be found, $t_a$ is the local minimum traveltime in the inside row, $t_b$ is the traveltime of the neighboring grid point at the source side, $s$ is the slowness at point $c$. However, if the term inside the square root of equation (7) is negative, the traveltime at point $c$ is computed as

$$t_c = t_a + hs \tag{8}$$

At the next stage, equation (4) is applied to compute traveltimes.

In application of equation (4), the propagation direction of local plane wave does not come in play. The traveltimes at the three corners $a$, $b$ and $d$ can also be used to compute the traveltime at corner $c$ because of the assumption of local plane wave. Equations (5) and (6) are then changed by computing the right hand side unknown traveltime from the left hand side known traveltime. However, it is easy to program calculation from small traveltimes to large traveltimes, i.e., in a upwind format.

Consider calculating traveltimes at side *1* (top) of Figure 4. Application of equation (4) is carried out in three loops. The first loop progresses from the left end to the lateral location of the source. Then the second loop progresses from the right end to the left end. Finally the third loop progresses from the lateral location of the source to the right end. During each loop, calculation starts at each local minimum traveltime point and progresses until a local maximum traveltime point is reached. Similar traveltime calculations are carried out sequentially for the other three sides.

## *EXAMPLE*

Figure 5(a) is a more complicated 1-D velocity model. Figure 5(b) shows the traveltime contours of direct arrivals with the source at the upper left corner. All the possible direct arrivals in 1-D medium are correctly modeled. It has transmission from high velocity medium to low velocity medium, transmission and creeping boundary wave from low velocity medium to high velocity medium, and overturning waves in medium with linear increasing velocities.

## *A POSTERIORI RAY TRACING*

After traveltimes are found for all the grid points, raypath from any receiver grid point back to the source can be traced by following the steepest descent direction through the traveltime field. The raypath is guaranteed to end at the source point as the source point has the smallest traveltime. Figure 6 shows the ray paths traced from the right edge of the model back to the source using the traveltime map of Figure 5(b).

## *DISCUSSIONS*

In this traveltime calculation scheme, the velocity model is parameterized as constant velocity cells. For one-dimensional velocity medium, it is perfect. For two-dimensional velocity medium, dipping interfaces are represented by stairways.

As seen in Figure 1, the calculated direct arrival traveltimes closely overlay the waveforms of wave equation modeling. We are confident that the direct arrival traveltimes calculated by our scheme are accurate up to the spatial and temporal sampling requirements.

The computational cost of this scheme at each grid point is to evaluate equation (7). For a model of realistic size, say 250,000 grid points, computational time is just a few seconds at a present workstation with computation speed of Mflops/s. Also traveltime computations are carried out in a few well defined loops as explained in the section of computation pattern, this traveltime computation scheme can easily put into a vector computer.

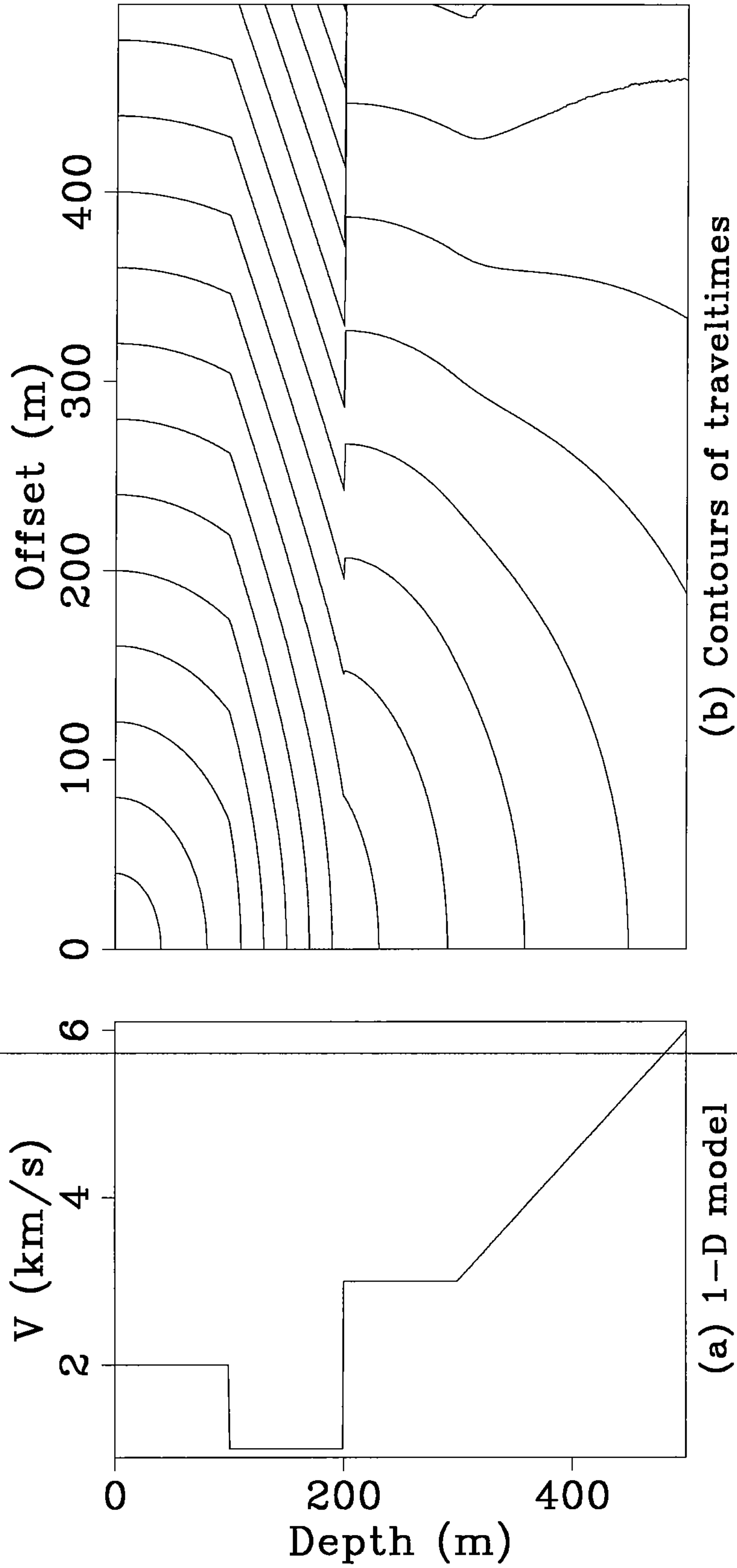


Figure 5: (a) is velocity model. (b) is the contours of direct arrival traveltimes.

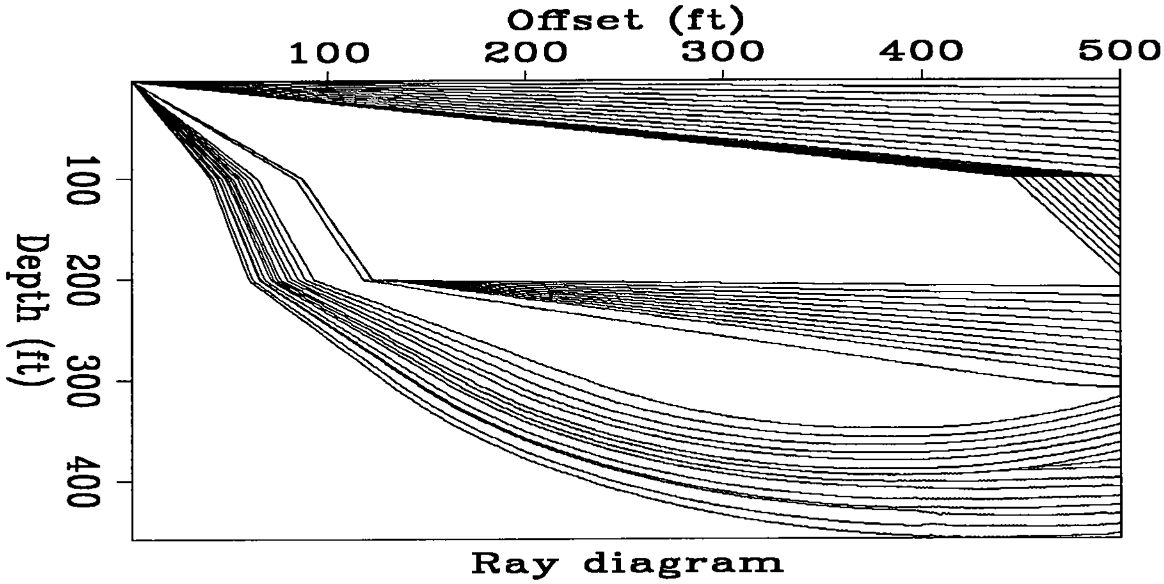


Figure 6: Raypaths from the right edge back to the source using the traveltime map of Figure 5(b).

## *CONCLUSIONS*

Our new scheme of finite-difference solving the eikonal equation successfully computes the traveltimes of direct arriving waves. The accuracy in computed traveltimes is good up to the spatial and temporal sampling requirements. Direct arrivals are usually the most energetic event in a time evolving wavefield. Traveltimes of direct arrivals will be very useful in both transmission traveltime tomography and migration imaging.

## *REFERENCES*

Cerveny, V., Molotkov, I. A., and Psencik, I., 1977, Ray method in seismology: Karlova Univerzita, Prague.

Podvin, P., and Lecomte, I., 1991, Finite difference computation of traveltimes in very contrasted velocity models: a massively parallel approach and its associated tools: Geophys. J. Int., **105**, 271–284.

Qin, F., Luo, Y., Oslen, K. B., Cai, W., and Schuster, G. T., 1992, Finite-difference solution of the eikonal equation along expanding wavefronts: Geophysics, **57**, 478–487.

Reshef, M., and Kosloff, D., 1986, Migration of common-shot gathers: Geophysics, **51**, 324–331.

Van Trier, J., and Symes, W. W., 1991, Upwind finite-difference calculation of traveltimes: Geophysics, **56**, 812–821.

Vidale, J., 1988, Finite-difference calculation of travel times: Bull. Seism. Soc. Am., **78**, no. 6, 2062–2076.

Vidale, J., 1990, Finite-difference calculation of travel times in 3-D: Geophysics, **55,** 521–526.

Zauderer, R., 1989, Partial Differential Equations of Applied Mathematics: John Wiley and Sons.

Zhang, L., 1993, Imaging by the wavefront propagation method: Ph.D. thesis, Stanford University.